THE JOURNAL OF PHYSICAL CHEMISTRY B

ARTICLE

pubs.acs.org/JPCB

Triplet−Triplet Annihilation in a Series of Poly(*p*-phenylene) Derivatives

Sebastian T. Hoffmann,[†] Jan-Moritz Koenen,[‡] Ullrich Scherf,[‡] Irene Bauer,[†] Peter Strohriegl,[§] Heinz Bässler,[†] and Anna Köhler*[,†]

[†]Experimental Physics II, University of Bayreuth, 95440 Bayreuth, Germany

[‡]Macromolecular Chemistry, Bergische Universität Wuppertal, 42097 Wuppertal, Germany

[§]Macromolecular Chemistry I, University of Bayreuth, 95440 Bayreuth, Germany

ABSTRACT: We have studied the temperature dependence of phosphorescence (Ph) and delayed fluorescence (DF) in two series of poly(*p*-phenylene) derivatives within a temperature range from 10 to 300 K under quasi-stationary conditions. One set of materials consists of the dimer, trimer, and polymer of ethylhexyl-substituted poly(fluorene) (PF2/6) and thus allows us to assess the effects of oligomer length. The second series addresses the influence of energetic disorder and conjugation length by being composed of the polymers alkoxy-substituted poly(*p*-phenylene) (DOO-PPP), poly(indenofluorene) (PIF), and ladder-type poly(*p*-phenylene) (MeLPPP). Under low light intensities, the DF features a maximum at a certain temperature T_{max}. For the dimer and trimer, the T_{max} coincides with the temperature at which the phosphorescence has decayed to 1/2 of the value at 10 K, while T_{max} shifts to lower temperature values along the series DOO-PPP, PIF, and MeLPPP and approaches T = 0 K for MeLPPP. By applying conventional kinetic equations we show that the occurrence of a maximum in the DF intensity is the consequence of generalized thermally activated triplet exciton transport toward quenching sites. We find the quenching rates at 0 K to be in the range of 1 s^{-1} for the polymers, while they are more than an order of magnitude lower for the oligomers.

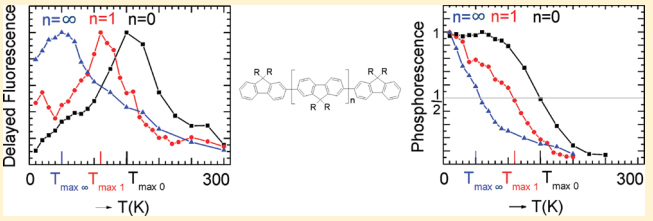

INTRODUCTION

Triplet states play a central role in the photophysical processes that control the operation of modern optoelectronic devices such as organic light emitting diodes (OLEDs) or organic solar cells containing π-conjugated oligomers and polymers as active elements. A large fraction of electron−hole recombination events in an OLED result in the formation of triplet states.[1,2] Unfortunately, they usually decay nonradiatively unless organometallic compounds are employed as efficient phosphorescence emitters.[3] In the latter case, any bimolecular process such as the reactions of two triplet excitations or quenching of a triplet excitation by charge carriers would be detrimental for the device efficiency.[4] A similar problem is encountered in organic solid state lasers.[5,6] Recall that the encounter of two triplet excitations with antiparallel spins generates one singlet state; i.e., one of the triplets is quenched.[1] Therefore, an efficient OLED needs to operate under conditions at which bimolecular triplet−triplet annihilation (TTA) is negligible.[7−12] The opposite condition applies to devices that operate in the fluorescence up-conversion mode, as has been suggested for solar cell applications.[13−16] In such a device, a fluorescent host material is doped by a triplet sensitizer with high intersystem crossing rate. The materials are chosen such that the energy of the singlet state in the host is above that of the sensitizer, while the ordering of the triplet levels is reversed. The host triplets that are generated via dopant sensitizing annihilate bimolecularly, and the dominant emission is delayed fluorescence of the host. In this case, TTA is the desired outcome, and any intervening quenching process that destroys the triplet excitations has to be avoided. These two examples illustrate the application-driven need to understand the kinetics associated with triplet excitations.

Apart from the obvious technological implications, studying the transport of triplet excitations in π-conjugated systems is an interesting and timely subject of research because it enables the gradual development of a full understanding of the transport of electronic excitations in disordered systems. For practical reasons, the materials employed in modern optoelectronic devices are usually noncrystalline. Structural randomness introduces specific features into the excitation dynamics.[17−21] Furthermore, triplet excitations migrate predominantly via short-range exchange interaction as charge carriers do. Therefore, they can serve as model objects for the understanding of charge transport.[1] In contrast to charge carriers, triplets have the advantage that they are amenable to photoluminescence spectroscopy and can thus be studied in a direct way.

The intensity of the phosphorescence (Ph) is determined by extrinsic quenching of triplet states with a rate k_q and by triplet−triplet annihilation (TTA) with a rate constant γ, in addition to the intrinsic radiative and nonradiative decay rate k_r and k_{nr}. TTA gives rise to delayed fluorescence (DF). Both

Received: March 24, 2011
Revised: May 31, 2011
Published: June 15, 2011

processes, Ph and DF, are temperature activated as they are controlled by the diffusion of triplet excitons. Triplet diffusion is governed by the product of a Marcus-type rate (polaronic controlled) and a Miller−Abrahams-type rate (disorder-controlled) and thus depends on material parameters such as the geometric reorganization energy (which changes with oligomer length) or energetic disorder.[20,22] In this work, we investigate how the temperature dependence of phosphorescence and delayed fluorescence depend on the temperature dependence of the quenching rate and TTA rate. We focus on the role of disorder and geometric relaxation energy in determining the rates of triplet diffusion and thus of quenching and annihilation. To this end, we employ two series of materials. In one series, the oligomer length is varied by using the dimer, trimer, and polymer of ethylhexyl-substituted poly(fluorene) (PF2/6). The second series consists of alkoxy-substituted poly(*p*-phenylene) (DOO-PPP), poly(indenofluorene) (PIF), and ladder-type poly(*p*-phenylene) (MeLPPP). These polymers all have a backbone made up by *p*-phenylenes, yet the number of stiffening links between *p*-phenylenes increases along the series thus gradually reducing the torsional degree of freedom. As a result, the conjugation length increases, while the energetic disorder decreases.[20]

EXPERIMENTAL SECTION

Poly[9,9-bis(2-ethylhexyl)fluorene] PF2/6 was synthesized via a standard homocoupling protocol after Yamamoto as described by Grell et al.[23] The sample investigated here had a weight average molecular weight M_w of ca. 160 kg/mol (M_n, 45 kg/mol; polydispersity index PDI, 3.56). The fluorene dimer and trimer were synthesized by a palladium-catalyzed Suzuki cross coupling as described in refs 24 and 25. Poly[6,6,12,12-tetra(2-ethylhexyl)-indenofluorene] (PIF) has been synthesized according to Setayesh et al.[26] with a weight-average molecular weight M_w of 400 kg/mol (M_n, 154 kg/mol; polydispersity index PDI, 2.60). The polymer was purified by repeated Soxhlet extractions with methanol, hexane, ethylacetate, dichloromethane, and chloroform. Poly(2,5-dioctyloxy-1,4-phenylene) (DOO-PPP) with a molecular weight of ca. 24.5 kg/mol (M_n, 14.5 kg/mol; PDI, 1.69) has been synthesized according to Huang et al.[27] The polymer was purified by repeated Soxhlet extractions with methanol, hexane, acetone, and ethylacetate. Methyl-substituted ladder-type poly(*p*-phenylene) (MeLPPP) has been synthesized according to Scherf et al.[28] with M_w of 66 kg/mol (M_n, 27 kg/mol; PDI, 2.44).

Films were spun cast from toluene solutions with concentrations of 20 mg/mL onto quartz substrates to a thickness of about 100−130 nm. The spectra were measured in a continuous flow helium cryostat, and the temperature was controlled by an Oxford Intelligent Temperature Controller (ITC-502). The excitation was provided by a pulsed, frequency-tripled Nd:YAG laser at 355 nm (3.49 eV) (Spectron SL401) with a pulse length of about 15 ns and repetition rates in the range of 0.8−10 Hz, depending on the lifetime of the phosphorescence. We took care to ensure that the time interval between two pulses was exceeding the phosphorescence lifetime. The light was detected by a time-gated intensified charge-coupled-device camera (Andor iStar DH734-18F-9AM). Measurements of phosphorescence intensity (I_{Ph}) and delayed fluorescence intensity (I_{DF}) were taken with a delay time of 500 ns. At each temperature, the gate was set to about four times the measured lifetime. This avoids errors due to integration of noise while still representing a measurement under steady state conditions.

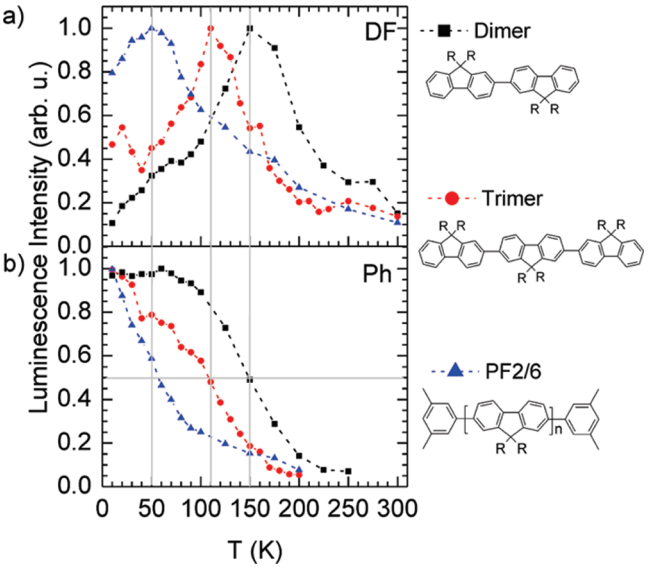

Figure 1. (a) Integrated delayed fluorescence spectra (DF) and (b) phosphorescence spectra (Ph) for PF2/6 polymer, trimer, and dimer as a function of temperature at an excitation density of 10 μJ/(cm^2 pulse). The dashed colored lines and the gray solid lines are guides to the eye. Also shown are the chemical structures. R = 2-ethylhexyl.

The measurements were taken at a low excitation density of 10 μJ cm^{-2} pulse^{-1} which corresponds to the monomolecular regime[20] and at a high excitation density of 1 mJ cm^{-2} pulse^{-1} which corresponds to the bimolecular regime. To increase the signal-to-noise ratio, all spectra at low excitation density were obtained by averaging over 500 laser shots at a particular delay time and for high excitation density over 200 laser shots.

RESULTS

Figure 1 shows how the intensity of phosphorescence (Ph) and delayed fluorescence (DF) change with temperature for a dimer, trimer, and polymer of PF2/6. When raising the temperature from 10 K onward, the delayed fluorescence first increases to a maximum intensity and then drops again. In contrast, the phosphorescence intensity, taken in the same shot by the iCCD camera, decreases monotonically. Three features are of interest. First, the delayed fluorescence has maximum intensity at a temperature T_{max} where the phosphorescence intensity is reduced to 1/2 of its value at 10 K. Second, this temperature T_{max} reduces with increasing length of the system; i.e., it is highest for the dimer and lowest for the polymer. Third, the ratio between the delayed fluorescence intensity at T_{max} and the delayed fluorescence intensity at $T = 0$, $[I_{DF}(T = T_{max})]/[I_{DF}(T = 0)]$, also reduces with increasing oligomer length.

While the data in Figure 1 serve to investigate the effect of oligomer length on T_{max}, in Figure 2, the consequences of energetic disorder and, concomitantly, of conjugation length are explored. The series of polymers DOOPPP, PIF, and MeLPPP are based on the same poly(*p*-phenylene) backbone, yet their rigidity increases along this series, implying a reduced energetic disorder and increased conjugation length. For this series of polymers, we observe that the temperature T_{max} for the maximum of delayed fluorescence reduces from DOOPPP to PIF, and it coincides with the 10 K intensity for MeLPPP. Like for the oligomers, the ratio $[I_{DF}(T = T_{max})]/[I_{DF}(T = 0)]$ reduces

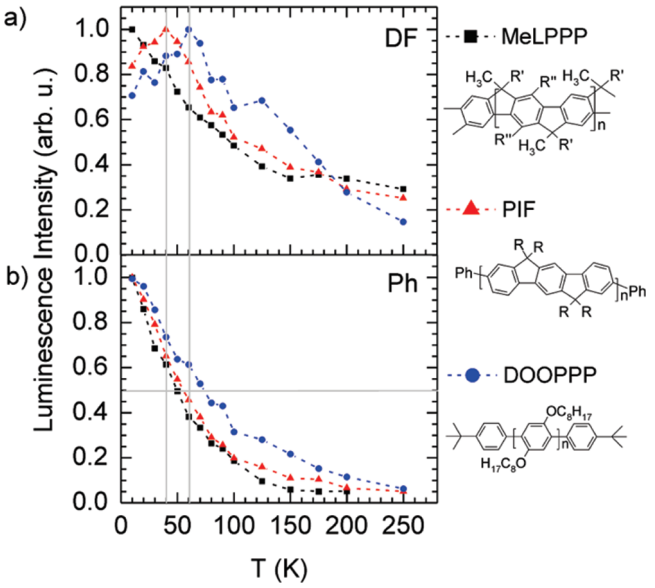

Figure 2. (a) Integrated delayed fluorescence spectra and (b) phosphorescence spectra for MeLPPP, PIF, and DOOPPP as a function of temperature at an excitation density of 10 μJ/(cm^2 pulse). The dashed colored lines and the gray solid lines are guides to the eye. Also shown are the chemical structures. R′ = 1,4-C_6H_4-n-$C_{10}H_{21}$ and R″ = -n-C_6H_{13}.

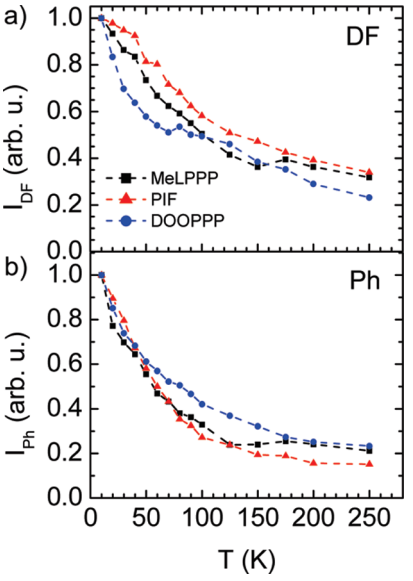

Figure 3. (a) Integrated delayed fluorescence (DF) and (b) phosphorescence (Ph) for MeLPPP, PIF, and DOOPPP as a function of temperature at an excitation density of 1 mJ/(cm^2 pulse). The dashed colored lines are guides to the eye.

with T_{max} along the series. Yet in contrast to the oligomers, for the polymers the phosphorescence intensity at the temperature T_{max} is larger than 1/2 of the 10 K value. More precisely, the value of the phosphorescence at T_{max} increases as T_{max} decreases.

These data give rise to a number of questions. It is not obvious why the delayed fluorescence should peak at a temperature where the phosphorescence has half its maximum value for short oligomers nor why this temperature might reduce with increasing oligomer length. Further, we wonder what causes a higher phosphorescence intensity at T_{max} in chemically very similar polymers. Finally, why do the trends in T_{max} and in $[I_{DF}(T = T_{max})]/[I_{DF}(T = 0)]$ correlate?

Before addressing these issues, we want to point out that the peak of delayed fluorescence can only be observed in the regime of low excitation intensity. This regime is defined by a linear increase of phosphorescence intensity with excitation power implying that the phosphorescence is controlled by a monomolecular process. The data presented in Figures 1 and 2 are taken in this linear low intensity regime. When the excitation intensity is high, bimolecular recombination processes dominate, and the phosphorescence intensity is proportional to the square root of the excitation power. In this case, the delayed fluorescence intensity exhibits no maximum with temperature. Rather, it decays continuously from 10 K onward. This is demonstrated in Figure 3 for the polymer series.

■ ANALYSIS

To get insight into these questions, we need to consider the rate equations for phosphorescence and delayed fluorescence. We start with the conventional rate equation for the concentration of triplet excitons under steady state conditions.

$$\frac{d[T]}{dt} = 0 = G - (k_r + k_{nr} + k_q)[T] - \gamma[T]^2 \qquad (1)$$

G is the rate of formation of triplet excitons by intersystem crossing from the singlet manifold. The decay rates of the triplet exciton by radiative decay, by intrinsic nonradiative decay (internal conversion), and by nonradiative quenching are given by k_r,k_{nr}, and k_q, respectively. γ is the rate constant for bimolecular triplet−triplet annihilation (TTA). The intensities of phosphorescence and delayed fluorescence are given by

$$I_{Ph} = k_r[T] \qquad (2)$$

$$I_{DF} = c\gamma[T]^2 \qquad (3)$$

In eq 3, the constant c is equal to the fraction of triplet−triplet encounters that generate a triplet state times the rate constant for radiative singlet decay. In the limit of low excitation density, eq 1 yields

$$[T] = \frac{G}{k_r + k_{nr} + k_q}, \ \gamma[T] \ll k_r + k_{nr} + k_q \qquad (4)$$

Inserting eq 4 into 2 and 3 gives

$$I_{ph} = \frac{k_r G}{k_r + k_{nr} + k_q} \qquad (5)$$

and

$$I_{DF} = \frac{c\gamma G^2}{(k_r + k_{nr} + k_q)^2} \qquad (6)$$

To determine the temperature T_{max} at which the delayed fluorescence has a maximum, we use the condition $(\partial)/(\partial T)I_{DF} = 0$. For the evaluation of this expression, we need to know the temperature dependence of the parameters involved. We take c, G, k_r, and k_{nr} to be independent of temperature, while we consider k_q and γ to vary with temperature. If we presume an Arrhenius-like temperature dependence for k_q and γ, we can

dx.doi.org/10.1021/jp202763e |J. Phys. Chem. B 2011, 115, 8417–8423

write

$$k_q(T) = k_{q0} + k_{q1} \exp\left(-\frac{E_{act}}{kT}\right) \quad (7)$$

and

$$\gamma(T) = \gamma_0 + \gamma_1 \exp\left(-\frac{E_{act}}{kT}\right) \quad (8)$$

While we discuss the justification for this in detail further below, we note here that triplet quenching and TTA are both controlled by the same kinetic process, i.e., the diffusion of triplet excitons. Consequently, k_q and γ are governed by the same general activation energy, and they can be considered to be proportional. This implies

$$\frac{k_{q1}}{\gamma_1} = \frac{k_{q0}}{\gamma_0} \quad (9)$$

Inserting eqs 7 and 8 into eq 6 and taking the derivative with respect to temperature, we arrive at

$$T_{max} = \frac{E_{act}}{k}\left[\ln \frac{k_{q1}\gamma_1}{(k_r + k_{nr} + k_q)\gamma_1 - 2k_{q1}\gamma_0}\right]^{-1} \quad (10)$$

Using eq 9, this can be simplified to

$$T_{max} = \frac{E_{act}}{k}\left[\ln \frac{k_{q1}}{(k_r + k_{nr}) - k_{q0}}\right]^{-1} \quad (11)$$

Equation 11 tells us that the temperature for the maximum intensity in delayed fluorescence, T_{max}, depends on the rate of quenching relative to the intrinsic decay rates k_r and k_{nr}. To derive the value of the phosphorescence intensity of $T = T_{max}$ relative to its value at $T = 0$, it is useful to evaluate eq 7 at both temperatures, yielding

$$k_q(T = 0) = k_{q0} \quad (12)$$

$$k_q(T = T_{max}) = k_r + k_{nr} \quad (13)$$

Thus, the delayed fluorescence has its maximum when the quenching rate equals the intrinsic decay rate. Inserting eqs 12 and 13 into eq 5, we find

$$\frac{I_{Ph}(T = T_{max})}{I_{Ph}(T = 0)} = \frac{1}{2}\frac{(k_r + k_{nr}) + k_{q0}}{k_r + k_{nr}} = \frac{1}{2}\left(1 + \frac{k_{q0}}{k_r + k_{nr}}\right) \quad (14)$$

Equation 14 is equal to 1/2 when $k_{q0} \ll k_r + k_{nr}$, i.e., when the quenching rate at 0 K is negligible compared to the intrinsic decay rate.

To address all the questions raised above, we still require the value of the delayed fluorescence maximum compared to the delayed fluorescence at 0 K. This requires evaluation of eq 8 at $T = 0$ and at $T = T_{max}$

$$\gamma(T = 0) = \gamma_0 \quad (15)$$

$$\gamma(T = T_{max}) = \frac{\gamma_0}{k_{q0}}(k_r + k_{nr}) \quad (16)$$

Inserting eqs 12, 13, 15, and 16 into eq 6 and employing eq 9 results in

$$\frac{I_{DF}(T = T_{max})}{I_{DF}(T = 0)} = \frac{1}{4}\left[\frac{(k_r + k_{nr})}{k_{q0}} + 2 + \frac{k_{q0}}{k_r + k_{nr}}\right] = \frac{1}{4}\frac{(k_r + k_{nr})}{k_{q0}}\left(1 + \frac{k_{q0}}{k_r + k_{nr}}\right)^2 \quad (17)$$

We have carried out these calculations assuming an Arrhenius-like temperature dependence for k_q and γ. It turns out that the relative intensities of Ph and DF given in eqs 14 and 17 are independent of the form of the temperature dependence assumed, provided that $k_q(T)$ and $\gamma(T)$ are thermally activated in a general form. For example, if in eqs 7 and 8 the exponential factor $\exp(-E_{act}/kT)$ is replaced by a factor $\exp(-(T_0/T)^2)$ that is characteristic for hopping within a Gaussian density of states distribution, eq 11 is transformed into

$$T_{max} = T_0\left[\ln \frac{k_{q1}}{(k_r + k_{nr}) - k_{q0}}\right]^{-0.5} \quad (18)$$

which then returns eqs 12−17 in the same form as above. In fact, any temperature dependence for k_q and γ in the general form "$c_1 + c_2 \exp(-g(T)/kT)$" (with c_1 and c_2 as constants and $g(T)$ an arbitrary function of temperature) will yield the same results. The key condition is that k_q and γ be proportional to each other. As both processes, the quenching of triplets and the annihilation of triplets, result from incoherent hopping of triplet excitons, it is a logical consequence that their temperature dependence should be proportional. This is also manifested in $\gamma = 8\pi\langle R\rangle D$, $\langle R\rangle$ being the reaction distance at which two triplets annihilate, and the diffusivity D is proportional to the rate constant for triplet exciton hopping.

In addition to reasoning, the temperature dependence of k_q and γ can simply be verified experimentally. Solving eq 5 for k_q yields

$$k_q(T) = \frac{k_r G}{I_{Ph}(T)} - (k_r + k_{nr}) \quad (19)$$

where we have now explicitly included the temperature dependence of k_q and I_{Ph} in our notation. If we define the phosphorescence intensity in the absence of quenching as $I_{Ph0} = k_r G(k_r + k_{nr})^{-1}$, we can write

$$k_q(T) = k_r G\left(\frac{1}{I_{Ph}(T)} - \frac{1}{I_{Ph0}}\right) \quad (20)$$

Equation 20 can be expressed in a different way. Since $k_r G I_{Ph}^{-1}(T) = \tau(T)$ and $k_r G I_{Ph0} = \tau_0$ (with $\tau = (k_r + k_{nr} + k_q)^{-1}$ being the triplet lifetime and $\tau_0 = (k_r + k_{nr})^{-1}$ being the triplet lifetime in the absence of quenching), we can write

$$k_q(T) = \frac{1}{\tau(T)} - \frac{1}{\tau_0} \quad (21)$$

While eq 20 relates the quenching rate to steady state intensity measurements, k_q is obtained from lifetime measurements in eq 21. Experimentally, determining $k_q(T)$ by eq 21 (as done in ref 20) is more exact than by eq 20 since phosphorescence lifetime measurements can be carried over a large dynamic range easily while the determination of the phosphorescence intensity with an iCCD camera becomes error-prone at elevated temperatures due to poor

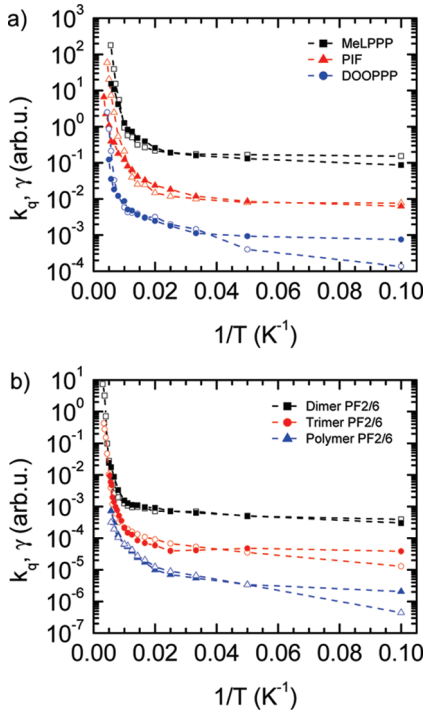

Figure 4. Rate constant for nonradiative quenching of triplet excitons k_q determined according to eq 21 (open symbols) and rate constant for bimolecular triplet−triplet annihilation γ determined according to eq 22 (filled symbols) as an Arrhenius plot for (a) MeLPPP, PIF, and DOOPPP and (b) PF2/6 dimer, trimer, and polymer. For the PF2/6 polymer, k_q is determined according to eq 20. The data for different materials are vertically offset for clarity of display.

signal-to-noise ratios. The bimolecular recombination constant can be obtained from solving eq 6

$$\gamma(T) = \frac{k_r^2}{c}\frac{I_{DF}(T)}{I_{Ph}^2(T)} \qquad (22)$$

In Figure 4, the temperature evolution of $k_q(T)$ and $\gamma(T)$ is compared. As expected, they are found in good agreement. In Figure 4, the k_q values have been taken from ref 20 for all materials except for the PF2/6 polymer. The PF2/6 polymer used in ref 20 had been purchased from American Dye Sources for convenience, yet it seemed to have a higher defect concentration than the other polymers. Therefore, for this manuscript, *all* polymers, including PF2/6, have been synthesized and purified by the Scherf group. For Figure 4, we have not repeated the time-consuming lifetime measurements on the Scherf PF2/6 but rather employed eq 20 to determine k_q.

Before applying these kinetic equations to our experimental data, we need to consider whether this approach is appropriate. In particular, we need to discuss whether the use of steady state kinetics is justified, although triplet diffusion is a dispersive process at low temperatures.[29,30] When considering the derivation outlined above, we find that an explicit time dependence only enters in eq 1 where it is assumed that the generation rate of triplet excitons equals their decay rate. Our experimental data were taken by applying an excitation pulse, waiting for 500 ns and then integrating all emissions. The time interval between two pulses was chosen to exceed the lifetime of the triplet exciton at each temperature. Thus, within the time interval Δt between two pulses, the decay is equal to the generation, and eq 1, i.e., $\Delta[T]/\Delta t = 0$, is fulfilled when integrating over many pulses. Thus, our experiments were conducted under quasi-steady state conditions.

Furthermore, it is worth keeping in mind that all measurements except those displayed in Figure 3 are taken in the limit of low excitation density ($\gamma[T] \ll k_r + k_{nr} + k_q$). Since k_q and γ are both based on the same underlying process of incoherent triplet exciton hopping, they are subject to the same evolution not only with respect to temperature but also with respect to time. In combination with the low excitation density, this should result in a similar progression of k_q and $\gamma[T]$ with time, implying that the ratio between monomolecular decay and bimolecular decay in eq 1 remains largely time independent, thus further entailing quasi-steady-state conditions.

DISCUSSION

After deriving the necessary kinetic equations and after evaluating their applicability, we can eventually turn to discussing the experimental data. Equations 11, 14, and 17 give us the expressions we need to address our initially outlined questions. Let us first consider what causes the peak in the temperature dependence of the delayed fluorescence intensity and how this relates to the phosphorescence intensity. From eq 13 we see that the DF peaks when the quenching rate equals the intrinsic decay rates. From Figure 4 we also know that k_q and γ are proportional and that they are temperature activated in some way. At first glance it may seem puzzeling that the DF exhibits a maximum, while γ and k_q both increase monotonically with temperature and at the same rate. The solution to this lies in the fact that the *rate*, by which the triplet concentration $[T]$ decays, is given by the product of the bimolecular decay constant times the triplet concentration, i.e., $\gamma[T]$ (see eq 3, $I_{DF} \propto (\gamma[T])[T]$). At low temperatures, when $k_q \ll k_r + k_{nr}$, $[T]$ is roughly constant with temperature, and the DF increases exponentially with γ, according to eq 3. However, when k_q exceeds $k_r + k_{nr}$, the triplet concentration is notably reduced by quenching (see eq 4), and thus the DF falls. In the limit of $k_q \gg k_r + k_{nr}$, it follows from eq 4 that $[T] \propto k_q^{-1}$, and since the DF is quadratic in the triplet concentration, DF decreases with k_q. This explains why the position of the peak in the DF intensity is a measure for the temperature at which triplet quenching equals the intrinsic triplet decay. Experimentally, we find this temperature T_{max} to reduce with oligomer length (Figure 1) and with reducing disorder of the polymers (Figure 2). This implies that triplet quenching becomes larger compared to the intrinsic decay rate with increasing oligomer length and with decreasing energetic disorder of the polymers.

To understand these trends, we need to take a closer look at the origin of the triplet quenching rate. The triplet quenching rate is obtained as a product of a triplet diffusion rate times an effective concentration of quenchers, $k_q = k_t c_q$. The effective concentration of quenchers is given by the number of quenching sites per volume times an interaction radius, over which they may quench a triplet. When no extrinsic quenchers are added, quenching sites may arise as oxidation products or from imperfect polymerization. A quenching reaction for triplets requires some wavefunction overlap to occur. As a result, the interaction radius of a quenching site occurring in a polymer with extended conjugated chromophores may be larger than that of a quencher in a short oligomer. Thus, the same number density of defect sites in two polymers of different conjugation length may result in a different *effective* quencher concentration.

For the delayed fluorescence to have a maximum, the quenching rate must be equal to a threshold value given by the sum of the intrinsic decay rates, i.e., $k_t c_q = k_r + k_{nr}$ (c.f. eq 13). If a material contains a large effective concentration of quenchers, the necessary quenching is already obtained for a low triplet diffusion rate. Since triplet diffusion is temperature activated of some kind, eq 13 is then fulfilled already at low temperature. Thus, for a material with a given triplet diffusion rate, T_{max} will reduce with increasing effective quencher concentration. Conversely, if C_q varies little within a set of materials, the temperature for obtaining the critical quenching rate reflects the temperature required for activating the triplet diffusion process. The faster the triplet diffusion, the lower T_{max}.

If we now compare the peaks in DF for the polymers and for the oligomers, we find that they occur at higher temperatures for the oligomers. This can be attributed to the superposition of both effects. First, it is generally known that oligomers are easier to purify than polymers; their synthesis tends to give rise to less defects than a polymerization reaction; and the interaction range of a defect in a short oligomer is small. Thus, the effective concentration of quenching sites in oligomers is smaller than in polymers. Second, electronic coupling for triplet diffusion between oligomers is small, and the thermal activation energy required to overcome the necessary geometric reorganization is large. For oligomers, triplet hopping requires electronic coupling through space, while some degree of through bond coupling can be operative along polymer chains. In addition, triplet diffusion in oligomers is dominated by the geometric reorganization energy, and the contribution of energetic disorder is negligible; this is not the case for polymers, in particular at temperatures around and below 100 K.[20,22] Thus, a comparatively poor triplet diffusion rate in combination with a higher purity of the material leads to a peak of delayed fluorescence at elevated temperatures in oligomers compared to related polymers.

Within the oligomer series, it is reasonable to presume a similar order of magnitude for the effective quencher concentration. The decrease of T_{max} with oligomer length then reflects mainly an increase in the triplet diffusion rate. This is consistent with the reduction in activation energy for triplet diffusion that has been observed as a function of oligomer length and that was attributed to a concomitant reduction in geometric reorganization energy.[20] A similar argument applies within the polymer series. With reducing energetic disorder, triplet diffusion increases both due to improved electronic coupling along the chain and due to a reduced need for activation energy. In addition, the concomitant increase in conjugation length implies an increased interaction range for quenching sites.

To summarize, the temperature for the maximum in DF reflects the relative magnitude of the triplet quenching process. The DF peak occurs at higher temperatures for the oligomers due to low triplet diffusion rates in combination with low effective defect concentration, while the converse is the case for polymers. We note that a maximum in the intensity of delayed fluorescence can only be obtained when a quenching process takes place with $0 < k_{q0} < (k_r + k_{nr})$. Without quenching sites, the delayed fluorescence rises monotonically. On the other hand, if the quenching rate at 0 K already exceeds the sum of the intrinsic decay rates, the delayed fluorescence continuously decreases from its 0 K value. This is the case for MeLPPP.

Let us now consider what we can learn from the intensity of the phosphorescence at the temperature where the delayed fluorescence peaks. Equation 14 tells us that the relative phosphorescence intensity is about 1/2 when the triplet quenching rate at 0 K is small compared to the intrinsic decay rate, say $(k_{q0})/(k_r + k_{nr}) \leq 0.1$. From Figure 1, this is evidently the case for the oligomers. Figure 2 shows us further that the relative phosphorescence intensity at T_{max} is larger than 1/2 for the polymers, with the deviation being larger for the more conjugated polymers. From eq 14 we find that this additional contribution arises when the triplet quenching rate at 0 K is a sizable fraction of the intrinsic decay rate. In fact, eq 14 can be used to determine that for DOO-PPP, PIF, and MeLPPP the ratio between k_{q0} and $(k_r + k_{nr})$ is 0.28, 0.36, and 1, respectively. Since the intrinsic lifetime $\tau_0 = (k_r + k_{nr})^{-1}$ of phosphorescence in PIF and MeLPPP tends to be on the order of 1 s (0.5 s for the alkoxy-substituted PPP), as determined from measurements in frozen solution,[31] this gives us a quantitative measure for the quenching rate in the absence of thermal activation at 0 K. Depending on the polymer, we find k_{q0} to be in the range of about $0.1-1\ s^{-1}$. For the oligomers, the relative phosphorescence intensity of 1/2 at the DF maximum tells us that the 0 K triplet quenching rate in oligomers is more than an order of magnitude lower than the intrinsic decay rate, or in absolute terms, k_{q0} can safely be estimated to be below $0.1\ s^{-1}$. The relative intensity of the DF peak, expressed through eq 17, follows the same trend. The DF intensity is large compared to the 0 K value when triplet quenching at 0 K is negligible, and it reduces as the 0 K quenching rate increases.

It is a remarkable observation that even without thermal energy we can observe triplet diffusion in a disordered system with poor electronic coupling such as an oligomer thin film. The triplet diffusion is evidenced by the existence of delayed fluorescence arising from triplet−triplet annihilation at very low temperatures. The occurrence of triplet hopping without thermal activation can be attributed to an energetic relaxation in the inhomogeneously broadened density of states.[32] Such a sequence of energetically downward hops will slow down with time in a $\ln(\ln(t))$ fashion, as fewer and fewer energetically lower sites are available, yet it will never stop entirely.[33] As a result, there is some, albeit small, triplet diffusion even at very low temperatures.

We now briefly consider why the delayed fluorescence intensity decreases from low temperatures onward without exhibiting a maximum when the excitation density is high (Figure 3). In the limit of very high excitation density, bimolecular recombination exceeds any other decay channel for the triplet. From eq 1, the triplet concentration can be derived as

$$[T] = \sqrt{\frac{G}{\gamma}} \qquad \gamma[T] \gg k_r + k_{nr} + k_q \tag{23}$$

Inserting eq 23 into eq 3 yields a constant intensity of the DF that is only controlled by the formation of triplet excitons.

$$I_{DF} = cG \tag{24}$$

Thus, if all triplets generated decay by triplet−triplet annihilation, the intensity of delayed fluorescence should be constant for all temperatures. The observation of a weak decrease in DF with temperature is due some temperature-activated quenching that consequently reduces the triplet concentration. This can also be seen in a quantitative fashion when solving the quadratic eq 1 for the triplet concentration $[T]$.

CONCLUSIONS

In summary, what can we learn from this? We have seen that the DF increases with temperature until the triplet quenching rate equals the intrinsic decay rates. From then onward, the DF falls since the triplet population is reduced by quenching. In between, a maximum forms. By measuring the temperature dependence of the DF and Ph, we can obtain information on the size of the triplet quenching rate relative to the intrinsic decay rate. For example, when the Ph is 1/2 of its 0 K intensity, triplet quenching at 0 K is negligible, while a value exceeding 1/2 is indicative of a 0 K quenching rate that is comparable to the intrinsic decay rate. This is observed for polymers, where tunneling events along a polymer chain can promote efficient triplet diffusion to quenching sites. In general, the DF peak occurs at higher temperatures for lower triplet quenching rates.

Applications exploiting triplet−triplet annihilation, such as the use of "incoherent triplet upconversion" for luminescence,[13−16] usually aim for intense delayed fluorescence with a maximum at room temperatures. In light of our results (in particular eq 3, eq 16, and eq 13), this asks for materials with a high triplet annihilation constant γ while keeping the 0 K triplet quenching rate k_{q0} low. Since γ is proportional to the triplet diffusion rate and k_{q0} is given by the product of 0 K triplet diffusion rate times effective quencher concentration, a reasonably large γ combined with a low k_{q0} can only be achieved by keeping the effective quencher concentration as low as possible. Keeping in mind that the effective quencher concentration is determined by the number density times the interaction range and that both factors tend to be larger in polymers than in oligomers, it appears that efficient room-temperature luminescence by triplet upconversion asks for using well-purified oligomers rather than polymers. The triplet diffusion rate required can then be optimized by varying the rigidity of the molecule (thus tuning the activation energy needed for diffusion) and the bulkiness of side chains (thus altering the size of the intermolecular electronic coupling). In a similar way, applications in OLEDs or organic lasing that require low TTA rates and low triplet-charge quenching rates at room temperature[7−12] will find this easier to obtain when using short oligomers instead of polymers and aiming for flexible rather than rigid backbones.

AUTHOR INFORMATION

Corresponding Author

*E-mail: anna.koehler@uni-bayreuth.de.

ACKNOWLEDGMENT

A.K. and P.S. acknowledge support from the Graduiertenkolleg Grako 1640 of the DFG.

REFERENCES

(1) Köhler, A.; Bässler, H. *Mater. Sci. Eng. R* **2009**, *66*, 71.
(2) Köhler, A.; Wilson, J. *Org. Electron.* **2003**, *4*, 179.
(3) Baldo, M. A.; O'Brien, D. F.; You, Y.; Shoustikov, A.; Sibley, S.; Thompson, M. E.; Forrest, S. R. *Nature* **1998**, *395*, 151.
(4) Hertel, D.; Meerholz, K. *J. Phys. Chem. B* **2007**, *111*, 12075.
(5) Gärtner, C.; Karnutsch, C.; Lemmer, U.; Pflumm, C. *J. Appl. Phys.* **2007**, *101*, 023107.
(6) Lehnhardt, M.; Riedl, T.; Weimann, T.; Kowalsky, W. *Phys. Rev. B* **2011**, *81*, 165206.
(7) Staroske, W.; Pfeiffer, M.; Leo, K.; Hoffmann, M. *Phys. Rev. Lett.* **2007**, *98*, 197402.
(8) Reineke, S.; Schwartz, G.; Walzer, K.; Leo, K. *Appl. Phys. Lett.* **2007**, *91*, 123508.
(9) Zang, F. X.; Sum, T. C.; Huan, A. C. H.; Li, T. L.; Li, W. L.; Zhu, F. *Appl. Phys. Lett.* **2008**, *93*, 023309.
(10) Luo, Y. C.; Aziz, H. *Adv. Funct. Mater.* **2010**, *20*, 1285.
(11) Lehnhardt, M.; Riedl, T.; Rabe, T.; Kowalsky, W. *Org. Electron.* **2011**, *12*, 486.
(12) Lebental, M.; Choukri, H.; Chenais, S.; Forget, S.; Siove, A.; Geffroy, B.; Tutis, E. *Phys. Rev. B* **2009**, *79*, 165318.
(13) Baluschev, S.; Miteva, T.; Yakutkin, V.; Nelles, G.; Yasuda, A.; Wegner, G. *Phys. Rev. Lett.* **2006**, *97*, 143903.
(14) Bagnich, S. A.; Bässler, H. *Chem. Phys. Lett.* **2003**, *381*, 464.
(15) Laquai, F.; Wegner, G.; Im, C.; Busing, A.; Heun, S. *J. Chem. Phys.* **2005**, *123*, 074902.
(16) Monguzzi, A.; Tubino, R.; Meinardi, F. *Phys. Rev. B* **2008**, *77*, 155122.
(17) Richert, R.; Bässler, H.; Ries, B.; Movaghar, B.; Grünewald, M. *Philos. Mag. Lett.* **1989**, *59*, 95.
(18) Rothe, C.; Monkman, A. P. *Phys. Rev. B* **2003**, *68*, 075208.
(19) Sudha Devi, L.; Al-Suti, M. K.; Dosche, C.; Khan, M. S.; Friend, R. H.; Köhler, A. *Phys. Rev. B* **2008**, *78*, 045210.
(20) Hoffmann, S. T.; Scheler, E.; Koenen, J. M.; Forster, M.; Scherf, U.; Strohriegl, P.; Bässler, H.; Köhler, A. *Phys. Rev. B* **2010**, *81*, 165208.
(21) Jankus, V.; Winscom, C.; Monkman, A. P. *J. Phys.: Condens. Matter* **2010**, *22*, 185802.
(22) Köhler, A.; Bässler, H. *J. Mater. Chem.* **2011**, *21*, 4003.
(23) Grell, M.; Knoll, W.; Lupo, D.; Meisel, A.; Miteva, T.; Neher, D.; Nothofer, H. G.; Scherf, U.; Yasuda, A. *Adv. Mater.* **1999**, *11*, 671.
(24) Thiem, H.; Jandke, M.; Hanft, D.; Strohriegl, P. *Macromol. Chem. Phys.* **2006**, *207*, 370.
(25) Thiem, H.; Rothmann, M. M.; Strohriegl, P. *Des. Monomers Polym.* **2005**, *8*, 619.
(26) Setayesh, S.; Marsitzky, D.; Mullen, K. *Macromolecules* **2000**, *33*, 2016.
(27) Huang, S. P.; Huang, G. S.; Chen, S. A. *Synth. Met.* **2007**, *157*, 863.
(28) Scherf, U.; Mullen, K. *Makromol. Chem., Rapid Commun.* **1991**, *12*, 489.
(29) Scheidler, M.; Cleve, B.; Bässler, H.; Thomas, P. *Chem. Phys. Lett.* **1994**, *225*, 431.
(30) Hoffmann, S. T.; Bässler, H.; Koenen, J. M.; Forster, M.; Scherf, U.; Scheler, E.; Strohriegl, P.; Köhler, A. *Phys. Rev. B* **2010**, *81*, 115103.
(31) Hertel, D.; Setayesh, S.; Nothofer, H. G.; Scherf, U.; Müllen, K.; Bässler, H. *Adv. Mater.* **2001**, *13*, 65.
(32) Movaghar, B.; Grunewald, M.; Ries, B.; Bässler, H.; Wurtz, D. *Phys. Rev. B* **1986**, *33*, 5545.
(33) Bässler, H. *Phys. Status Solidi B* **1993**, *175*, 15.